ISSN 0915-633X

NATIONAL INSTITUTE FOR FUSION SCIENCE

Recovery of Cesium in the Hydrogen Negative Ion Sources

Yu.I. Belchenko, Y. Oka, O. Kaneko, Y. Takeiri, A. Krivenko, M. Osakabe, K. Tsumori, E. Asano, T. Kawamoto and R. Akiyama

(Received - Oct. 15, 1999)

NIFS-621 Dec. 1999

RESEARCH REPORT
NIFS Series

NAGOYA, JAPAN

Recovery of Cesium in the Hydrogen Negative Ion Sources

Yu.I.Belchenko[1)], Y.Oka[2)], O.Kaneko[2)], Y.Takeiri[2)], A.Krivenko[1)],
M Osakabe[2)], K.Tsumori[2)], E Asano[2)], T.Kawamoto[2)], R.Akiyama[2]

[1)] Budker Institute of Nuclear Physics, Novosibirsk, 630090, Russia
[2)]National Institute for Fusion Science, Toki-city, 509-5292, Japan

Abstract.
Cesium recovery from the polluted layers in the 1/3 scale hydrogen negative ion source for LHD-NBI system has tested. It was found, that the cesium recovery can be produced by additional discharges as from the cesium layer, aged by tungsten and residual gas, so as from the cesium layers, polluted by an occasional water leak. The highest cesium recovery to NI production was produced by a xenon arc, while glow discharge and arcing in hydrogen were less effective. The mechanism of recovery is the ejection of cesium from the underlying enriched layer by the arc and its transport to the surface.

Keywords: hydrogen negative ion, recovery of cesium, ion source, NBI, Cs-W

A number of multicusp negative ion sources developed for neutral beam injection into fusion devices have explored seeding of cesium[1]. Most of the seeded cesium in the developed versions of the multicusp sources is buried with the evaporated tungsten on the water-cooled internal surfaces of gas-discharge box[2]. It seems important to recover the cesium, buried on the discharge chamber walls instead of just additional feed. We have tested the cesium recovery from the polluted layers by additional discharges in the 1/3 scale hydrogen negative ion source for LHD-NBI system. The results of cesium recovery experiments are described below.

Experimental Setup

In cesium recovery experiments, an External-filter-type 1/3 scale Multicusp NI source (EMS) was used, which has been developed for high-energy and high-current NI beam production[1]. The tungsten filaments are used in the source for electron emission. A direct deposition of cesium was done to EMS inner walls with a small movable oven[2]. There are three grids used for H^- beam extraction and acceleration - Plasma Grid (PG), extraction grid and grounded grid. The PG has 270 apertures of 9 mm in diameter. The ion source is attached to the NBI test stand[1]. The H^- beam acceleration up to 90 keV with beam pulse duration 0.6-1.3 s was used. A multichannel calorimeter, located 11.2 m downstream from the ion source is used for H^- ion current measurement. About 2.5 A H^- current produced with the 1/3 scale source at 50 kW arc power is to be scaled up to 40 A H^- yield for the full-scale source[1].

Cesium recovery was produced by an additional discharges during the 30-60 min pause in EMS operation. For recovery of cesium on the Plasma Chamber (PC) wall the last one was acting as a cathode of additional discharge. PG surface recovery was done with PG acting as a cathode. A 0.4-0.6 kV voltage provides the xenon glow ignition. A glow-to-arc transition occurs with the glow current increase, and a pulsed arc discharges were supported in the xenon or hydrogen. The arc current and pulse duration were depended on cesium coverage thickness and were decreased with the cesium depletion. A regular EMS discharge in hydrogen and xenon, using an electron emission from the EMS filaments was also tested for cesium recovery. The PC or PG was biased to the cathode potential during this PC or PG processing by the EMS discharge. A special electrodes were introduced onto the PC wall for ignition the vacuum arc. Attempts to ignite the vacuum arc on the cesiated PC surface were launched after the 0.1 g cesium deposition by cesium plasma, but they failed.

Cesium recovery from Cs-W coverage

A. Deposition of small cesium amount into the EMS produces the temporal increase of H^- current for several pulses of source operation[2]. Fig.1 shows the evolution of H^- current from shot to shot (triangles, left scale), and arc power of shot (circles, right scale) in the case of 10 mg cesium deposition and its processing by an additional discharges. H^- current was increased to a value of 1.3 A after the cesium deposition to PC back (done before the shot # 60) and it was decreased with the further operation due to cesium blocking (Fig.1).

An attempt to recover the blocked cesium by a xenon glow was done before the shot # 89 in Fig.1. A dc glow (0.3 kV/0.5 A) at xenon pressure 0.5 Pa was applied during about 20 minutes with PC acting as a cathode. A negligible change of H^- yield was recorded after this (shots # 95-98 in Fig.1). The next processing was done with PC acting as an arc cathode (PC arcing). About 10^2 pulsed arcs were ignited at xenon pressure 0.8-1.5 Pa before shots #98. It results in a temporal increase of H^- current to 0.5 A value, but then H^- current was decreased fast (Fig.1). PG processing with PG acting as an arc cathode (PG arcing) was done then. About 10^2 pulsed arcs were ignited with the PG having a cathode potential at xenon pressure 1.5 Pa before shot #110. No improvement of H^- yield was recorded after PG arcing (Fig.1). Fig.1 shows, that cesium recovery is inefficient in the case of small cesium deposition.

B. Deposition of 0.1-0.2 g Cs portions while using an optimal amount of filaments in the discharge demonstrates the stable enhancement of H^- yield for a longer period of source operation[2]. Namely, 0.1 g deposition provides the increase of H^- beam current to 2.8 A value, and it was slowly degraded down to 2 A level in 500 shots/2 days of operation The next 0.15 g deposition produces the 2.8 A level of H^- current and it was decreased down to 1.7 A during 600 shots/4 days operation (at discharge power about 50 kW, hydrogen pressure 0.7 Pa, 8 filaments). Several types of additional discharges were tested for H^- production recovery after this cesium blocking. Fig.2 show the H^- current evolution before and after these EMS processing (triangles, left scale), and an arc power of corresponding shot (circles, right scale).

1. PC arcing was produced at xenon pressure of about 0.7 Pa before shot #1232. After producing about $2\cdot10^2$ pulsed arcs (20-30 A, 5-15 msec) the H^- production was tested again. H^- current was increased up to 2.3 A with the PG temperature growth to 160-170 ^{0}C, and it was decreased to the previous value 1.7 A during the further 50 shots/ 2 hours operation (Fig.2). No one breakdown happened during the source high-voltage operation after the cesium recovery processing in xenon.

2. Attempt to recover the cesium-tungsten layer on PG surface was done by the PG biasing to the cathode potential while the source was operated in the regular EMS arc mode with hydrogen feed and electron emission from heated filaments. After producing the 9 pulses with PG at cathode bias (arc power 5-10 kW, shots # 1287-95 in Fig.2) the H^- production was checked again. H^- yield had a value of 0.8 A at PG starting temperature 80 ^{0}C, it was increased to 1.5 A level with the PG temperature growth to 220 ^{0}C, and had no change with the further operation and PG heating up to 260 ^{0}C (Fig.2). No temporal peak of H^- production was recorded

in this case The H^- current steady-state level was about 0.2 A lower, than it was before the PG processing with PG cathode biasing in the EMS regular arc!

3 The processing by the regular EMS arc with the PC biasing to the cathode potential was tested next The arc in xenon was used, since an attempt to ignite the arc in hydrogen with the PC biasing to the cathode was failed 13 pulses of EMS regular arc (40-60 A/60 V) were produces at xenon pressure 0 7 Pa. The H^- yield had about the same value after this PC processing, as it was before.

4. About $2\cdot10^2$ pulsed arcs were produced during the PC arcing at hydrogen pressure 5-10 Pa. The H^- beam current had about 7-10% increased value after PC arcing in hydrogen, and it was degraded down to the previous value after 50 shots/2 hours operation.

5. About 30 minute PC processing as a cathode of 1 kV/ 1-3 mA dc glow in hydrogen had no changed the H^- yield.

6. About $2\cdot10^3$ pulsed arcs (10-20 A, 40-80 V, 5-20 msec) were produced during the next PC arcing at xenon pressure 0.5-3 Pa. This more intense PC arcing results in a more steady 30% H^- yield increase and the following slower decrease down to the previous value during the 70 shot/2.5 hours operation. The next intense PC arcing was applied after an additional 0.1 g cesium deposition to PC and its aging by a 400 shot/3 day operation. About 10^3 pulsed arcs (20-30 A, 30-75 V, 5-10 msec) were produced at xenon pressure 0.7 Pa. It resulted in a steady 25% increase of H^- current up to 2.5 A level with a following slow decrease down to the previous value during about 10^2 shot /3 hours of further operation. A 30% H^- current increase to 2.2 A level was recorded after the next PC arcing, produced 3 days later. Several intense PC arcings provide the steady 25-30% H^- yield enhancement, but H^- current absolute value was higher after arcing of EMS coverage, enriched by cesium.

Cesium recovery from a water-polluted layer

The cesium recovery from the cesium-tungsten layer, polluted by an occasional water leak was tested as well. About 0.6 g of cesium was deposited to the PC surface during 700 shots of EMS operation, preceding the occasional water leak. The evolution of H^- beam current due to cesium recovery procedures from the water-polluted layer is shown in Fig.3. The H^- beam current had a value of 0.5 A at arc power 50 kW and gas filling pressure 0.7 Pa after the source pollution with a water leak. This value was about 20-30% higher, than H^- yield from the pure hydrogen discharge.

About 10^3 pulsed arcs with the PG as an arc cathode, and then about $5\cdot10^2$ pulsed arcs with the PC as an arc cathode were produced at xenon pressure 1.5 Pa. After this processing, done before the shot #1 in Fig.3, the H^- current was increased up to 1.1 A at the 10^{th} shot, and then was decreased to the previous value 0.5 A after about 20 shots/ 40 min of operation. The next PC and/or PG arcing processing in xenon displayed approximately the same evolution of H^- current (Fig.3). The second PC arcing (10^3 arc pulses) was done before shot # 35 at xenon pressure 2 Pa. The increase of H^- current up to 1.4 A level was displayed (shot #48 in Fig.3). After about $5\cdot10^3$ arcs produced with PG biased to the cathode potential (before shot #56) the H^- current was increased to a maximal value 1 2 A (shot #66). The next arcing processing, produced on the water-polluted PC and PG surface (before shot #78) have resulted in the same temporal increase of H^- current to 1.1 A (shots #86-92). PG optimal temperature was about 140-190 ^{0}C at H^- current maximum. No trace of electrode erosion by PC/PG multiple arcing was detected on EMS surfaces after the source evacuation to atmosphere.

The listed data shows, that several arcing processing on water-polluted electrodes produces the same temporal 2-fold enhancement of H^- yield, but does not recover the optimal cesium-tungsten coverage on PG surface completely. As a result, the H^- current maximum after the water-polluted electrodes processing was about two times less, than that after a thick Cs-W coverage arcing. The enhanced H^- yield degraded 2-3 times faster after the water-polluted electrode recovery (or after cesium adding to water-polluted electrodes[2]), as compared with that after the Cs-W coverage arcing. It shows, that cesium deposited on the water-polluted layer provides a smaller replenishment flux to PG surface.

DISCUSSION

The data obtained evinces the cesium blocking on the PC/PG walls and its recovery for H^- production by an additional discharge processing. The highest cesium recovery were produced by arcing in xenon, while arcing in hydrogen and processing by glow were less effective. The principle of cesium recovery by arc is the decomposition of cesium compound, the cesium ejection from the underlying layer and the renewal of the cesium coverage on EMS surfaces. The internal layer of Cs-W reservoir are enriched by cesium, so the arc ejection of electrode material increases the percentage of cesium in the coverage. An arc ejects of about 1 atom of cathode material per 10 cathode emitted electrons, so the EMS processing with 10^3 arcs (10^{-2} s, 30 A) evaporates of about 30 mg of Cs-W coverage. Cesium recovery is less efficient for a higher tungsten percentage in the coverage.

PC arcing can produce the Cs^+ ion implantation to PG coverage with positive ion flux to the arc anode. The ejection of the overlayed tungsten by arcing and the tungsten sputtering by glow is also important for the improvement of cesium seed from the buried layer.

Our data demonstrates the importance of optimal PG coverage structure for H^- production enhancement. A minute PG processing by a regular EMS hydrogen discharge with PG biasing to the cathode produces a sizable decrease of H^- current (Fig.2). It can be caused by H^- production decrease due to Cs-W coverage loading with energetic hydrogen ions[3]. The pollution of Cs+W coverage by a water leak increases the PG work function and stops the replenishment flux to PG It decreases the H^- production down to about pure hydrogen level.

The cesium recovery can be produced by vacuum arcing on the thick Cs-W coverage. Vacuum arc supplies an intense (10% of arc current) flux of energetic positive ions to the anode and can produce Cs^+ ion implantation to PG coverage. The H^- extraction voltage applying during the arcing will prevent the Cs^+ flux to the extraction gap. It is proposed to support the cesium recovery *in situ* by applying the pulsed arcing/glowing within the pause between the injector pulses.

Cesium recovery processing in xenon produces an easy flux of cesium to PG surface and does not decrease the electrical strength of extraction/acceleration gaps. The xenon filling to PC during the standard cesium deposition procedure can also decrease the cesium flux to accelerator and to improve the high-voltage holding-on of the EMS. The cesiated hollow cathodes or RF discharge can be used instead of the hot tungsten filaments for EMS feeding with plasma.

SUMMARY

Optimal PG cesium coverage structure is important for H^- production enhancement. Cesium blocking by evaporated tungsten decreases the H^- yield from the EMS. Electrode processing by an additional discharge recovers the H^- production. The mechanism of recovery is the ejection of cesium from the underlying enriched layer by arc and it transport to the surface. Recovery processing permits the use of deposited cesium more efficiently and to minimize cesium addition during the EMS longterm operation.

Literature

1. O.Kaneko, Y.Oka, M.Osakabe, Y.Takeiri, K.Tsumori, R,Akiyama, E.Asano, T.Kuroda and A.Ando. Proceedings of the 16th Symposium on Fusion Engineering, Vol.2 (1995), p.1082
2. Y.Oka, Y.Takeiri, Yu.Belchenko, M.Hamabe, O.Kaneko, K.Tsumori, M.Osakabe, E.Asano, T.Kawamoto, R.Akiyama. Rev.Sci.Instrum., this issue.
3. J.J.Geerlings, P.W. van Amersfoort, L.F.Kwakman, E.H.Granneman, J.Los, and J.P.Gauyacq, Surf. Sci., **157**, 151(1985)

Figure Captions

Fig 1. H- current evolution after 10 mg Cs deposition and PC/PG arcing.

Fig.2 H- current evolution after PC arcing and after PG processing by EMS discharge in hydrogen.0.25 g cesium deposited

Fig.3. H- current evolution after water-polluted electrodes arcing.

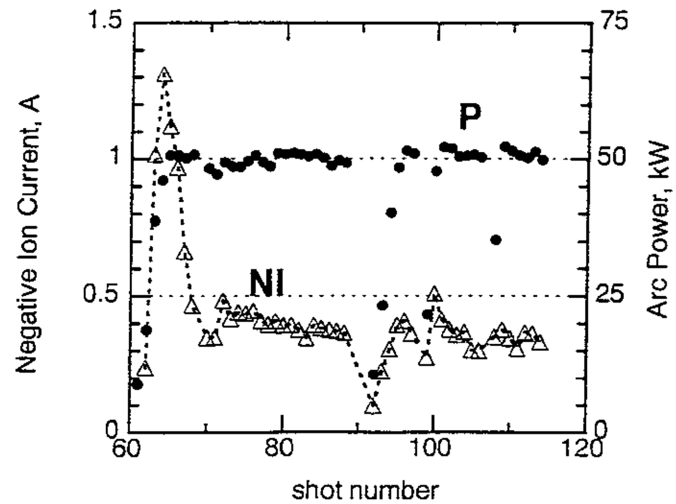

Fig.1. H- current evolution after 10 mg Cs deposition and PC/PG arcing

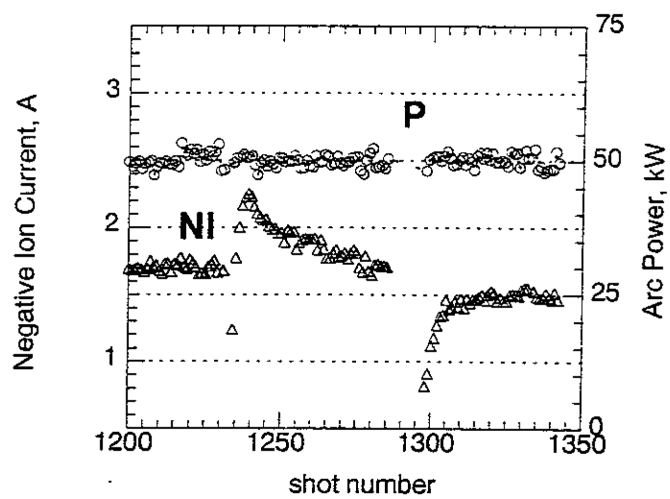

Fig.2. H- current evolution after PC arcing and after PG processing by EMS discharge in hydrogen.0.25 g cesium blocked.

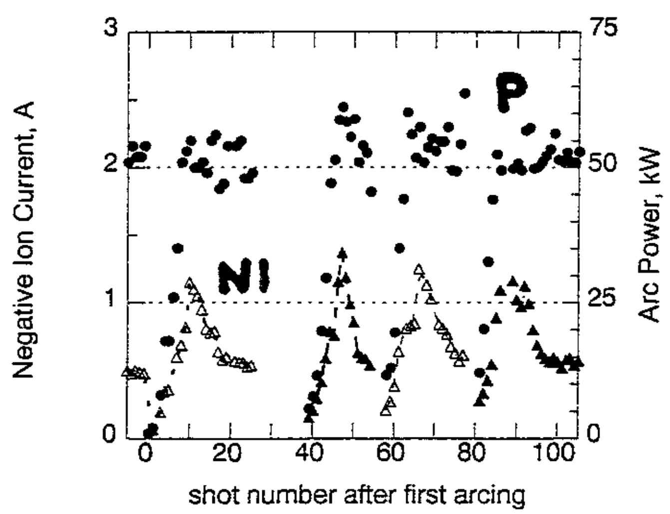

Fig.3 H- current evolution after water-polluted electrodes arcing

Recent Issues of NIFS Series

NIFS-559 R Horiuchi, K Nishimura and T Watanabe,
Kinetic Stabilization of Tilt Disruption in Field-Reversed Configurations; Sep 1998
(IAEA-CN-69/THP1/11)

NIFS-560 S Sudo, K. Kholopenkov, K Matsuoka, S Okamura, C Takahashi, R Akiyama, A Fujisawa, K Ida, H Idei, H Iguchi, M Isobe, S Kado, K. Kondo, S Kubo, H Kuramoto, T Minami, S Morita, S Nishimura, M Osakabe, M Sasao, B Peterson, K Tanaka, K Toi and Y Yoshimura,
Particle Transport Study with Tracer-Encapsulated Solid Pellet Injection; Oct 1998
(IAEA-CN-69/EXP1/18)

NIFS-561 A. Fujisawa, H Iguchi, S Lee, K Tanaka, T Minami, Y Yoshimura, M Osakabe, K Matsuoka, S. Okamura, H Idei, S Kubo, S Ohdachi, S Morita, R Akiyama, K. Toi, H Sanuki, K Itoh, K Ida, A Shimizu, S. Takagi, C Takahashi, M Kojima, S Hidekuma, S Nishimura, M. Isobe, A. Ejiri, N. Inoue, R. Sakamoto, Y. Hamada and M Fujiwara,
Dynamic Behavior Associated with Electric Field Transitions in CHS Heliotron/Torsatron, Oct 1998
(IAEA-CN-69/EX5/1)

NIFS-562 S Yoshikawa,
Next Generation Toroidal Devices; Oct. 1998

NIFS-563 Y Todo and T. Sato,
Kinetic-Magnetohydrodynamic Simulation Study of Fast Ions and Toroidal Alfvén Eigenmodes; Oct 1998
(IAEA-CN-69/THP2/22)

NIFS-564 T. Watari, T. Shimozuma, Y Takeiri, R. Kumazawa, T. Mutoh, M. Sato, O Kaneko, K Ohkubo, S. Kubo, H. Idei, Y. Oka, M Osakabe, T. Seki, K Tsumori, Y. Yoshimura, R. Akiyama, T. Kawamoto, S. Kobayashi, F. Shimpo, Y Takita, E. Asano, S Itoh, G Nomura, T. Ido, M. Hamabe, M. Fujiwara, A Iiyoshi, S. Morimoto, T. Bigelow and Y.P Zhao,
Steady State Heating Technology Development for LHD, Oct 1998
(IAEA-CN-69/FTP/21)

NIFS-565 A. Sagara, K.Y. Watanabe, K Yamazaki, O. Motojima, M. Fujiwara, O. Mitarai, S. Imagawa, H Yamanishi, H. Chikaraishi, A Kohyama, H. Matsui, T. Muroga, T. Noda, N. Ohyabu, T. Satow, A.A. Shishkin, S Tanaka, T. Terai and T Uda,
LHD-Type Compact Helical Reactors, Oct 1998
(IAEA-CN-69/FTP/03(R)

NIFS-566 N. Nakajima, J. Chen, K. Ichiguchi and M Okamoto,
Global Mode Analysis of Ideal MHD Modes in L=2 Heliotron/Torsatron Systems, Oct 1998
(IAEA-CN-69/THP1/08)

NIFS-567 K Ida, M. Osakabe, K. Tanaka, T. Minami, S Nishimura, S. Okamura, A. Fujisawa, Y Yoshimura, S. Kubo, R Akiyama, D S Darrow, H Idei, H. Iguchi, M. Isobe, S. Kado, T. Kondo, S. Lee, K. Matsuoka, S. Morita, I Nomura, S Ohdachi, M Sasao, A Shimizu, K. Tumori, S. Takayama, M. Takechi, S Takagi, C. Takahashi, K Toi and T. Watari,
Transition from L Mode to High Ion Temperature Mode in CHS Heliotron/Torsatron Plasmas; Oct 1998
(IAEA-CN-69/EX2/2)

NIFS-568 S. Okamura, K Matsuoka, R. Akiyama, D S. Darrow, A. Ejiri, A. Fujisawa, M. Fujiwara, M. Goto, K Ida H. Idei, H Iguchi, N. Inoue M Isobe, K. Itoh, S. Kado, K Khlopenkov, T. Kondo, S. Kubo, A. Lazaros, S. Lee, G. Matsunaga, T Minami, S. Morita, S Murakami, N. Nakajima, N Nikai, S. Nishimura, I. Nomura, S. Ohdachi, K. Ohkuni, M. Osakabe, R. Pavlichenko, B Peterson, R Sakamoto, H. Sanuki, M. Sasao, A. Shimizu, Y Shirai, S. Sudo, S Takagi, C Takahashi, S. Takayama, M Takechi, K Tanaka, K Toi, K. Yamazaki, Y Yoshimura and T Watari,
Confinement Physics Study in a Small Low-Aspect-Ratio Helical Device CHS; Oct 1998
(IAEA-CN-69/OV4/5)

NIFS-569 M M Skoric, T Sato, A. Maluckov, M.S. Jovanovic,
Micro- and Macro-scale Self-organization in a Dissipative Plasma, Oct 1998

NIFS-570 T Hayashi, N Mizuguchi, T-H Watanabe, T. Sato and the Complexity Simulation Group,
Nonlinear Simulations of Internal Reconnection Event in Spherical Tokamak; Oct 1998
(IAEA-CN-69/TH3/3)

NIFS-571 A. Iiyoshi, A. Komori, A. Ejiri, M. Emoto, H. Funaba, M Goto, K. Ida, H Idei, S. Inagaki, S Kado, O. Kaneko, K Kawahata, S Kubo, R. Kumazawa, S Masuzaki, T Minami, J. Miyazawa, T. Morisaki, S. Morita, S Murakami, S Muto, T Muto, Y Nagayama, Y Nakamura, H Nakanishi, K. Narihara, K. Nishimura, N Noda, T. Kobuchi, S. Ohdachi, N. Ohyabu, Y. Oka, M Osakabe, T. Ozaki, B.J Peterson, A. Sagara, S Sakakibara, R. Sakamoto, H Sasao, M. Sasao, K Sato, M Sato, T Seki, T. Shimozuma, M Shoji, H. Suzuki, Y. Takeiri, K. Tanaka, K Toi, T Tokuzawa, K Tsumori, I. Yamada, H Yamada, S. Yamaguchi, M Yokoyama, K Y.Watanabe, T. Watari, R. Akiyama, H. Chikaraishi, K Haba, S. Hamaguchi, S. Iima, S. Imagawa, N. Inoue, K Iwamoto, S Kitagawa, Y. Kubota, J Kodaira, R. Maekawa, T Mito, T. Nagasaka, A. Nishimura, Y. Takita, C Takahashi, K Takahata, K Yamauchi, H. Tamura, T. Tsuzuki, S Yamada, N. Yanagi, H. Yonezu, Y Hamada, K Matsuoka, K. Murai, K. Ohkubo, I Ohtake, M Okamoto, S Sato, T Satow, S. Sudo, S. Tanahashi, K Yamazaki, M. Fujiwara and O Motojima,
An Overview of the Large Helical Device Project; Oct 1998
(IAEA-CN-69/OV1/4)

NIFS-572 M. Fujiwara, H Yamada, A. Ejin, M. Emoto, H. Funaba, M. Goto, K. Ida, H. Idei, S. Inagaki, S. Kado, O Kaneko, K. Kawahata, A. Komori, S Kubo, R. Kumazawa, S. Masuzaki, T. Minami, J. Miyazawa, T. Morisaki, S. Morita, S. Murakami, S Muto, T. Muto, Y. Nagayama, Y. Nakamura, H. Nakanishi, K. Narihara, K. Nishimura, N. Noda, T. Kobuchi, S Ohdachi, N Ohyabu, Y Oka, M. Osakabe, T Ozaki, B. J. Peterson, A. Sagara, S. Sakakibara, R. Sakamoto, H. Sasao, M. Sasao, K Sato, M Sato, T Seki, T. Shimozuma, M. Shoji, H. Sazuki, Y. Takeiri, K. Tanaka, K. Toi, T. Tokuzawa, K. Tsumori, I. Yamada, S. Yamaguchi, M. Yokoyama, K.Y. Watanabe, T. Watari, R. Akiyama, H. Chikaraishi, K. Haba, S. Hamaguchi, M. Iima, S. Imagawa, N. Inoue, K. Iwamoto, S. Kitagawa, Y. Kubota, J Kodaira, R. Maekawa, T. Mito, T. Nagasaka, A. Nishimura, Y. Takita, C Takahashi, K. Takahata, K. Yamauchi, H. Tamura, T. Tsuzuki, S. Yamada, N. Yanagi, H. Yonezu, Y. Hamada, K. Matsuoka, K Murai, K. Ohkubo, I. Ohtake, M. Okamoto, S. Sato, T. Satow, S. Sudo, S. Tanahashi, K. Yamazaki, O Motojima and A Iiyoshi,
Plasma Confinement Studies in LHD; Oct. 1998
(IAEA-CN-69/EX2/3)

NIFS-573 O. Motojima, K. Akaishi, H. Chikaraishi, H. Funaba, S. Hamaguchi, S. Imagawa, S Inagaki, N. Inoue, A. Iwamoto, S. Kitagawa, A. Komori, Y. Kubota, R. Maekawa, S. Masuzaki, T. Mito, J. Miyazawa, T. Morisaki, T. Muroga, T. Nagasaka, Y Nakmura, A. Nishimura, K. Nishimura, N. Noda, N Ohyabu, S. Sagara, S. Sakakibara, R Sakamoto, S. Satoh, T. Satow, M. Shoji, H Suzuki, K. Takahata, H. Tamura, K. Watanabe, H. Yamada, S. Yamada, S. Yamaguchi, K. Yamazaki, N. Yanagi, T. Baba, H Hayashi, M. Iima, T Inoue, S. Kato, T Kato, T. Kondo, S. Moriuchi, H Ogawa, I. Ohtake, K. Ooba, H Sekiguchi, N Suzuki, S Takami, Y. Taniguchi, T Tsuzuki, N Yamamoto, K Yasui, H Yonezu, M. Fujiwara and A Iiyoshi,
Progress Summary of LHD Engineering Design and Construction, Oct. 1998
(IAEA-CN-69/FT2/1)

NIFS-574 K. Toi, M. Takechi, S. Takagi, G. Matsunaga, M. Isobe, T. Kondo, M. Sasao, D.S. Darrow, K. Ohkuni, S. Ohdachi, R Akiyama A. Fujisawa, M. Gotoh, H. Idei, K. Ida, H. Iguchi, S Kado, M. Kojima, S. Kubo, S. Lee, K. Matsuoka, T. Minami, S Morita, N. Nikai, S. Nishimura, S. Okamura, M. Osakabe, A. Shimizu, Y. Shirai, C. Takahashi, K. Tanaka, T. Watari and Y. Yoshimura,
*Global MHD Modes Excited by Energetic Ions in Heliotron/Torsatron Plasmas,*Oct. 1998
(IAEA-CN-69/EXP1/19)

NIFS-575 Y Hamada, A Nishizawa, Y. Kawasumi, A. Fujisawa, M. Kojima, K. Narihara, K Ida, A. Ejin, S. Ohdachi, K. Kawahata, K Toi, K. Sato, T Seki, H. Iguchi, K. Adachi, S. Hidekuma, S.Hirokura, K. Iwasaki, T. Ido, R. Kumazawa, H Kuramoto, T Minami, I. Nomura, M. Sasao, K.N. Sato, T. Tsuzuki, I. Yamada and T. Watari,
*Potential Turbulence in Tokamak Plasmas;*Oct 1998
(IAEA-CN-69/EXP2/14)

NIFS-576 S. Murakami, U. Gasparino, H. Idei, S. Kubo, H. Maassberg, N. Marushchenko, N Nakajima, M. Romé and M. Okamoto,
*5D Simulation Study of Suprathermal Electron Transport in Non-Axisymmetric Plasmas;*Oct. 1998
(IAEA-CN-69/THP1/01)

NIFS-577 S. Fujiwara and T. Sato,
Molecular Dynamics Simulation of Structure Formation of Short Chain Molecules; Nov 1998

NIFS-578 T. Yamagishi,
Eigenfunctions for Vlasov Equation in Multi-species Plasmas Nov. 1998

NIFS-579 M. Tanaka, A. Yu Grosberg and T. Tanaka,
Molecular Dynamics of Strongly-Coupled Multichain Coulomb Polymers in Pure and Salt Aqueous Solutions;Nov. 1998

NIFS-580 J. Chen, N. Nakajima and M. Okamoto,
*Global Mode Analysis of Ideal MHD Modes in a Heliotron/Torsatron System: I. Mercier-unstable Equilibria;*Dec. 1998

NIFS-581 M. Tanaka, A. Yu Grosberg and T. Tanaka,
Comparison of Multichain Coulomb Polymers in Isolated and Periodic Systems: Molecular Dynamics Study; Jan 1999

NIFS-582 V.S. Chan and S. Murakami,
Self-Consistent Electric Field Effect on Electron Transport of ECH Plasmas; Feb 1999

NIFS-583 M. Yokoyama, N. Nakajima, M. Okamoto, Y Nakamura and M. Wakatani,
*Roles of Bumpy Field on Collisionless Particle Confinement in Helical-Axis Heliotrons;*Feb. 1999

NIFS-584 T.-H. Watanabe, T. Hayashi, T. Sato, M. Yamada and H. Ji,
*Modeling of Magnetic Island Formation in Magnetic Reconnection Experiment;*Feb. 1999

NIFS-585 R. Kumazawa, T. Mutoh, T. Seki, F. Shinpo, G. Nomura, T Ido, T. Watari, Jean-Marie Noterdaeme and Yangping Zhao
Liquid Stub Tuner for Ion Cyclotron Heating;Mar. 1999

NIFS-586 A. Sagara, M. Iima, S. Inagaki, N. Inoue, H. Suzuki, K. Tsuzuki, S. Masuzaki, J. Miyazawa, S. Morita, Y. Nakamura, N. Noda, B.

Peterson, S Sakakibara, T Shimozuma, H Yamada, K Akaishi, H Chikaraishi, H Funaba, O Kaneko, K Kawahata, A Komori N Ohyabu, O Motojima, LHD Exp Group 1, LHD Exp Group 2,
Wall Conditioning at the Starting Phase of LHD, Mar 1999

NIFS-587 T Nakamura and T Yabe,
Cubic Interpolated Propagation Scheme for Solving the Hyper-Dimensional Vlasov-Poisson Equation in Phase Space, Mar 1999

NIFS-588 W.X Wnag, N. Nakajima, S Murakami and M Okamoto,
An Accurate δf Method for Neoclassical Transport Calculation, Mar 1999

NIFS-589 K Kishida, K Araki, S. Kishiba and K Suzuki,
Local or Nonlocal? Orthonormal Divergence-free Wavelet Analysis of Nonlinear Interactions in Turbulence, Mar. 1999

NIFS-590 K. Araki, K. Suzuki, K. Kishida and S Kishiba,
Multiresolution Approximation of the Vector Fields on T^3, Mar 1999

NIFS-591 K. Yamazaki, H Yamada, K.Y Watanabe, K Nishimura, S Yamaguchi, H. Nakanishi, A Komori, H. Suzuki, T. Mito, H. Chikaraishi, K. Murai, O Motojima and the LHD Group,
Overview of the Large Helical Device (LHD) Control System and Its First Operation, Apr 1999

NIFS-592 T Takahashi and Y Nakao,
Thermonuclear Reactivity of D-T Fusion Plasma with Spin-Polarized Fuel, Apr 1999

NIFS-593 H. Sugama,
Damping of Toroidal Ion Temperature Gradient Modes, Apr 1999

NIFS-594 Xiaodong Li ,
Analysis of Crowbar Action of High Voltage DC Power Supply in the LHD ICRF System; Apr 1999

NIFS-595 K. Nishimura, R. Horiuchi and T Sato,
Drift-kink Instability Induced by Beam Ions in Field-reversed Configurations; Apr 1999

NIFS-596 Y. Suzuki, T-H. Watanabe, T. Sato and T. Hayashi,
Three-dimensional Simulation Study of Compact Toroid Plasmoid Injection into Magnetized Plasmas; Apr 1999

NIFS-597 H. Sanuki, K. Itoh, M. Yokoyama, A. Fujisawa, K. Ida, S. Toda, S.-I. Itoh, M. Yagi and A Fukuyama,
Possibility of Internal Transport Barrier Formation and Electric Field Bifurcation in LHD Plasma May 1999

NIFS-598 S. Nakazawa, N. Nakajima, M. Okamoto and N. Ohyabu,
One Dimensional Simulation on Stability of Detached Plasma in a Tokamak Divertor, June 1999

NIFS-599 S. Murakami, N. Nakajima, M. Okamoto and J. Nhrenberg,
Effect of Energetic Ion Loss on ICRF Heating Efficiency and Energy Confinement Time in Heliotrons, June 1999

NIFS-600 R. Horiuchi and T Sato,
Three-Dimensional Particle Simulation of Plasma Instabilities and Collisionless Reconnection in a Current Sheet,, June 1999

NIFS-601 W. Wang, M Okamoto, N. Nakajima and S. Murakami,
Collisional Transport in a Plasma with Steep Gradients; June 1999

NIFS-602 T. Mutoh, R. Kumazawa, T Saki, K Saito, F. Simpo, G Nomura, T. Watari, X. Jikang, G. Cattanei, H Okada, K. Ohkubo, M. Sato, S. Kubo, T. Shimozuma, H Idei, Y. Yoshimura, O Kaneko, Y Takeiri, M. Osakabe, Y Oka, K Tsumori, A Komori, H Yamada, K Watanabe, S Sakakibara, M Shoji, R. Sakamoto, S Inagaki, J Miyazawa, S. Morita, K Tanaka, B.J. Peterson, S Murakami, T Minami, S. Ohdachi, S. Kado, K. Narihara, H. Sasao, H Suzuki, K Kawahata, N. Ohyabu, Y Nakamura, H Funaba, S Masuzaki, S. Muto, K. Sato, T. Morisaki, S. Sudo, Y Nagayama, T Watanabe, M Sasao, K . Ida, N Noda, K Yamazaki, K Akaishi, A Sagara, K. Nishimura, T. Ozaki, K Toi, O. Motojima, M. Fujiwara, A. Iiyoshi and LHD Exp Group 1 and 2,
First ICRF Heating Experiment in the Large Helical Device, July 1999

NIFS-603 P.C. de Vries, Y Nagayama, K. Kawahata, S. Inagaki, H Sasao and K. Nagasaki,
Polarization of Electron Cyclotron Emission Spectra in LHD, July 1999

NIFS-604 W. Wang, N. Nakajima, M. Okamoto and S. Murakami,
δf Simulation of Ion Neoclassical Transport; July 1999

NIFS-605 T. Hayashi, N. Mizuguchi, T. Sato and the Complexity Simulation Group,
Numerical Simulation of Internal Reconnection Event in Spherical Tokamak, July 1999

NIFS-606 M. Okamoto, N. Nakajima and W. Wang,
On the Two Weighting Scheme for δf Collisional Transport Simulation; Aug. 1999

NIFS-607 O. Motojima, A.A. Shishkin, S. Inagaki, K. Y. Watanabe,
Possible Control Scenario of Radial Electric Field by Loss-Cone-Particle Injection into Helical Device; Aug. 1999

NIFS-608 R. Tanaka, T. Nakamura and T. Yabe,
Constructing Exactly Conservative Scheme in Non-conservative Form, Aug. 1999

NIFS-609 H. Sugama,
Gyrokinetic Field Theory; Aug. 1999

NIFS-610 M. Takechi, G. Matsunaga, S. Takagi, K.Ohkuni, K. Toi, M. Osakabe, M. Isobe, S. Okamura, K. Matsuoka, A. Fujisawa, H. Iguchi, S. Lee, T. Minami, K. Tanaka, Y. Yoshimura and CHS Group,
Core Localized Toroidal Alfven Eigenmodes Destabilized By Energetic Ions in the CHS Heliotron/Torsatron, Sep. 1999

NIFS-611 K. Ichiguchi,
MHD Equilibrium and Stability in Heliotron Plasmas; Sep. 1999

NIFS-612 Y. Sato, M. Yokoyama, M. Wakatani and V. D. Pusovitov,
Complete Suppression of Pfirsch-Schluter Current in a Toroidal l=3 Stellarator; Oct. 1999

NIFS-613 S. Wang, H. Sanuki and H. Sugama,
Reduced Drift Kinetic Equation for Neoclassical Transport of Helical Plasmas in Ultra-low Collisionality Regime; Oct. 1999

NIFS-614 J. Miyazawa, H. Yamada, K. Yasui, S. Kato, N., Fukumoto, M. Nagata and T. Uyama,
Design of Spheromak Injector Using Conical Accelerator for Large Helical Device, Nov. 1999

NIFS-615 M. Uchida, A. Fukuyama, K. Itoh, S.-I. Itoh and M. Yagi,
Analysis of Current Diffusive Ballooning Mode in Tokamaks; Dec. 1999

NIFS-616 M. Tanaka, A.Yu Grosberg and T. Tanaka,
Condensation and Swelling Behavior of Randomly Charged Multichain Polymers by Molecular Dynamics Simulations; Dec. 1999

NIFS-617 S. Goto and S. Kida,
Sparseness of Nonlinear Coupling; Dec. 1999

NIFS-618 M.M. Skoric, T. Sato, A. Maluckov and M.S. Jovanovic,
Complexity in Laser Plasma Instabilities Dec. 1999

NIFS-619 T.-H. Watanabe, H. Sugama and T. Sato,
Non-dissipative Kinetic Simulation and Analytical Solution of Three-mode Equations of Ion Temperature Gradient Instability; Dec. 1999

NIFS-620 Y. Oka, Y. Takeiri, Yu.I Belchenko, M. Hamabe, O. Kaneko, K. Tsumori, M. Osakabe, E. Asano, T. Kawamoto, R. Akiyama,
Optimization of Cs Deposition in the 1/3 Scale Hydrogen Negative Ion Source for LHD-NBI System ;Dec 1999

NIFS-621 Yu.I. Belchenko, Y. Oka, O. Kaneko, Y. Takeiri, A. Krivenko, M. Osakabe, K. Tsumori, E. Asano, T. Kawamoto, R. Akiyama,
Recovery of Cesium in the Hydrogen Negative Ion Sources, Dec 1999